Late and progressive alterations of sleep dynamics following central thalamic deep brain stimulation (CT-DBS) in chronic minimally conscious state

Zoe M. Adams,[1] Peter B. Forgacs,[1,2] Mary M. Conte,[1] Tanya J. Nauvel,[1] Jonathan D. Drover,[1] and Nicholas D. Schiff[1,2]

1 Feil Family Brain and Mind Research Institute, Weill Cornell Medical College, 1300 York Avenue, New York, NY

2 The Rockefeller University, 1230 York Avenue, New York, NY

Corresponding author:
Nicholas D. Schiff, MD
Weill Cornell Medical College
1300 York Avenue
Laboratory of Cognitive Neuromodulation
Department of Neurology
New York, NY
10065
Voice: 212-746-2372
Fax: 212-746-8050
Email: nds2001@med.cornell.edu

Conflict of Interest Statement:

None of the authors have potential conflicts of interest to be disclosed.

Acknowledgment:

This work was supported by NIH grant # HD91512, the James S. McDonnell Foundation, and the Jerold B. Katz Foundation.

1. Introduction

We report changes in sleep dynamics recorded in the electroencephalogram (EEG) from a 44 year-old male patient subject (PS) in association with central thalamic deep brain stimulation (CT-DBS). The PS had a long-standing history of severe traumatic brain injury (TBI) occurring at the age of 17 and has remained in a minimally conscious state (MCS) since the time of injury. CT-DBS began 21 years after injury, and sleep EEG measurements were obtained prior to implantation and followed longitudinally over three and a half years post-implantation.

The possible significance of the presence or absence of specific sleep elements as well as their evolution over time is not well characterized in minimally conscious state patients. Patients in MCS exhibit intermittent evidence of responsiveness without the ability to communicate due to lack of consistent or goal-directed movements to external stimuli (Giacino et al. 2002). Compared to patients in the vegetative state (VS), many MCS patients have hallmark features of sleep, such as spindles and slow waves (Landsness et al. 2011). However, these elements are often indistinct and challenging to identify according to the normal criteria for sleep staging in persons without brain injury (Cologan et al. 2010). Rare examples of late recovery have revealed the potential for cognitive capacity in some patients (Voss et al. 2006). Thus, the examination of longitudinal fluctuations in sleep electrophysiology may provide insight into otherwise unmeasured changes in overall brain function.

The examination of sleep in the setting of CT-DBS is warranted because two key elements of healthy sleep—spindles and slow waves—are generated via thalamocortical feedback loops that prominently involve the neurons within the central thalamus (Contreras et al. 1997; David et al. 2013). CT-DBS has been proposed as a method to drive frontostriatal activity in the underactive, widely deafferented brain to facilitate behavioral recovery (Schiff et al. 2007). After severe structural brain injuries such as the one observed in our PS, widespread deafferentation can be expected to produce broad disfacilitation of large-scale cerebral networks (Gold and Lauritzen 2002). The central thalamus has been proposed to play a key role in the maintenance of synaptic activity across the frontostriatal systems during wakeful states following severe brain injuries (Schiff, N.D., 2012; 2010). In support of this hypothesis, CT-DBS produced behavioral improvements in one minimally conscious patient six years after injury (Schiff et al. 2007). Additionally, cortical evoked responses in this patient provided direct evidence of CT-DBS activation of fronto-central cortical regions (Schiff et al. 2007). While our PS did not show overt behavioral improvements as a result of CT-DBS, the changes in sleep dynamics observed from pre- to post-CT-DBS implantation provide insight into electrophysiological consequences of CT-DBS treatment.

2. Methods

We collected the following longitudinal data presented here as part of a continuing in-patient study of patients with severe brain injury in recovery from disorders of consciousness (DOC). Written consent was obtained from the patient's surrogate.

2.1 Study participants

This PS participated separately as one of three subjects in a first-in-man study of CT-DBS effects in MCS (Schiff et al. 2007; Giacino et al. 2012). This patient has been studied longitudinally at four separate time points: first 1 month before DBS implantation (Time point 1, TP 1), second 23 months after DBS (Time point 2, TP 2), third 42 months after DBS (Time point 3, TP 3), and fourth approximately 60 months after DBS (Time point 4, TP 4) (Figure 1). The PS' medications did not change over the five-year period studied. As measured with the Coma Recovery Scale-Revised (CRS-R), the PS did not show overt behavioral improvements at the bedside post-CT-DBS (CRS-R scores ranged from 11-14 over the course of four visits spanning a five-year period); therefore, he was determined to be in MCS at each admission. See Supplement A for a full clinical history. The healthy volunteer (HV) is a 36 year-old age-matched female who was admitted to our study twice, with six months between each visit. We obtained one overnight sleep study from the HV at each admission. The HV gave written consent and was compensated for participation at the end of each study visit.

2.2 Data acquisition

For the PS, we recorded the overnight EEG at each of the above admissions. We obtained continuous video-EEG recordings during all PS admissions, which include one overnight sleep study at the first and second admissions and two consecutive nights on the third and fourth admissions. For the HV, we obtained continuous 24-hour video-EEG recordings during two admissions, and determined there were no significant differences between spectra obtained from the first and second admissions. Thus, we present results from the HV's first admission.

Scalp electrodes were placed according to the International 10-20 system (TP 1; 30 electrodes, TPs 2, 3, 4 and HV recording; 37 electrodes). The EEG was recorded using the Natus XLTEK EEG (San Carlos, CA). In addition, EOG electrodes were placed at right and left outer canthi to record eye movements. Review of the synchronous video record assured the eyes were closed through the entire portion of the record used for analysis. Impedances measured at the beginning and periodically during the recordings were $\leq$ 5 kOhms.

2.3 CT-DBS Methods

See Schiff et al. 2007 for general methods of CT-DBS surgery and implantation. The cycling of the stimulator was set to a 12 hours ON/12 hours OFF cycle (ON: 6 A.M. – 6 P.M.).

2.4 EEG analysis

2.4.1 Selection of epochs for power spectral analysis

Visual inspection of the sleep EEG record at the first admission revealed abnormal elements (Figure 1, TP 1). Specifically, an unusual mixing of sleep features, which are normally associated with distinct sleep stages, was observed at the first time point pre-CT-DBS. We identified periods of sleep at this pre-CT-DBS time point as either ***"stage 2-like"*** or ***"SWS-like,"*** and we selected epochs for power spectral analysis from each category. **"*SWS-like*"** segments at the first time point included low frequency (delta) waves with a constant intrusion of slow spindle-like and stage 2-like low amplitude activity (Figure 1, TP 1, blue arrow). While spindles may be present in the SWS of HVs, they are typically sparse and do not occur over prolonged periods in SWS. Periods identified as ***"stage 2-like"*** exhibited stage 2-like components, including partially formed spindles or slow spindles (~8-9 Hz) (Figure 1, TP 1, red arrow). K-complexes, a common feature seen in HV stage 2 sleep, were not present in the sleep record of this PS. To quantify the extent of the mixing at the pre-CT-DBS time point, we chose the most extreme versions of the **"*SWS-like*"** and **"*stage 2-like*"** stages for spectral analysis. For post-CT-DBS time points, the same approach to categorization was taken, although visual inspection of the record showed more clear separation of SWS periods from Stage 2.

2.4.2 Power spectral analysis

For both the PS and HV, we selected eyes-closed, artifact-free segments from a visual review of the sleep EEG record between the hours of 10pm and 6am. We sampled representative segments from different parts of the night. For the third and fourth PS admissions, representative segments of stage 2 and SWS from both overnight sleep studies were selected after having been plotted separately to ascertain whether spectral features were similar between nights. For the HV data, we selected and concatenated stage 2 (spindles and K-complexes) and SWS segments from one overnight study at one admission. Power spectral analysis was performed in MATLAB (The Mathworks, Natick, MA). For both PS and HV data, multi-taper (5 tapers) power spectral estimates were calculated using an Hjorth Laplacian montage on 30-35 10-second segments (Thomson 1982; Percival and Walden 1993; Mitra and Pesaran 1999), as implemented by the code mtspectrumc in the Chronux toolbox (Bokil et al. 2010).

2.4.3 Quantification of power spectra

Sleep spindle size in each patient visit was normalized using the methods from Gottselig, Bassetti, & Achermann (2002). For the stage 2 and SWS segments, we fit a power law function to each power spectra in the ranges from 5-6 and 17-18 Hz and 5-6 and 13-14 Hz, respectively. We then subtracted the fitted value at 6-18 Hz for stage 2 segments and 6-13 Hz for SWS segments, which allowed us to find the peak spindle frequency and amplitude as well as the peak power in the spindle range in SWS (Figure 2C). These ranges encompass both slow and fast spindling (slow spindles: 9-12 Hz; fast spindles: 12-15 Hz; Mölle, Bergmann, Marshall, & Born, 2011).

2.4.4 Time-frequency spectrogram analysis

The EEG was partitioned into 3-second non-overlapping segments. We obtained multi-taper spectral estimates (Thomson 1982) from each 3-second segment (5 tapers per segment) to window the data. The Fast Fourier transform of each tapered data segment was computed using the fftw3 libraries (Frigo and Johnson 2005). Tapered estimates of the power spectral density (PSD) were averaged within each epoch. The spectrograms show the 10*log values of the power spectrum of each of these segments.

2.5 Sleep scoring

In the HV, we scored sleep according to standard clinical neurophysiological descriptions (American Clinical Neurophysiology Society, Guideline 7). In the PS, sleep scoring index values were identified using an approach defined from a larger cohort of MCS patients in Forgacs et al. (2014) to produce a full sleep architecture (hypnogram): **Awake:** Eyes-open awake, **Stage 1:** included vertex waves defined as large amplitude (50-150 μV) delta sharp transients maximal over the vertex (central, midline electrodes), **Stage 2:** included spindle-like formations with amplitudes of 20-100 μV across fronto-central channels with a frequency of 8.5 to 15 Hz as well as K-complexes, **Slow wave sleep (SWS):** included large (> 50 μV) polymorphic delta (< 4 Hz) waves over 20% of any 30-second epoch. Some epochs, especially during the pre-CT-DBS time point, may have included large delta waves with smaller spindle-like formations interspersed among the delta waves, and **rapid eye movement (REM) sleep:** included lower-voltage activity on the EEG in conjunction with total absence of myogenic artifacts. Patient was behaviorally sleeping with eyes closed and there was evidence of a faster (theta to alpha) rhythm. Importantly, sleep was scored as REM when these behavioral and EEG features were present even at times when typical rapid eye movements were not observed. Since this PS had eye movement abnormalities during wakeful states as well, we did not consider lack of typical rapid eye movements an exclusion criteria for a state to be designated as REM. Nonetheless, this PS did exhibit occasional short bursts of rapid lateral eye movements during times that were otherwise scored as REM (Supplemental Figure 2), corroborating the appropriateness of our EEG and behavioral criteria as detailed above.

A fellowship-trained clinical neurophysiologist (P.B.F.) scored the PS' and HV's sleep at each admission. Sleep was scored from the hours of 10pm to 6am per 30-second epoch. The lights were off in the patient's room during these hours of the night. We created hypnograms from: 1) one overnight study from the first night of the patient's first admission (only one overnight sleep study was obtained at this time point), 2) the second night of two overnight sleep studies from the patient's fourth admission, and 3) one overnight study during the HV's first admission.

3. Results

We identified four changes in the patient's sleep arising across the pre-CT-DBS to post-CT-DBS time points: 1) increased segregation of stage 2 and SWS spectral features, 2) an increase in spindling frequency in stage 2, 3) a decrease in peak power in the spindle range in SWS, and 4) the emergence of REM sleep starting at TP 3 post-CT-DBS.

3.1 Segregation of sleep stages

We quantify the abnormal patterns of stage 2 and SWS features observed in the sleep EEG (Figure 1, see Methods) using power spectra obtained from these two states (Figure 2A). The "***slow-wave-sleep (SWS)-like*"** stage in the pre-CT-DBS sleep data not only show a low frequency component in the delta frequency range (~0.5 Hz), but also a ~9 Hz frequency component. The latter falls within the expected range for slow spindles (9-12 Hz; Mölle et al., 2011). This intrusion of spindling activity into SWS is seen not only in this channel but in 26 of 30 total channels. The HV SWS spectra (blue lines, right column) demonstrate a peak in the delta frequency range ~2 Hz and do not contain a spindle peak.

Power spectra from the ***"stage II-like"*** stage in the pre-CT-DBS data show a broad peak centered at ~8.7 to 9.5 Hz across 26 of 30 total channels. There were no K-complexes observed during stage 2 sleep within the PS data. The HV spectra (right column) illustrate a spindle peak ~14 Hz in Stage 2 only. The low frequency peak ~2 Hz in the stage 2 spectrum likely represents a K-complex.

Figure 2A further illustrates the segregation of sleep stages that occurs from the pre-CT-DBS time point to the last time point (TP 4) post-CT-DBS. At the pre-CT-DBS time point, stage 2 and SWS contain similar spectral features in both low frequency and spindling ranges (left column). Stage 2 (red line) and SWS (blue line) spectra overlap from 2-6 Hz, and the SWS spectrum contains a slow spindle-like peak ~9 Hz. At TP 4 post-CT-DBS, the stages show separate features with the loss of the spindle peak ~9 Hz in the SWS spectrum (blue lines, middle column) and a slight increase in low frequency power in the 2-6 Hz range. We observe the loss of the ~9 Hz peak in the SWS spectrum starting at TP 2, and the power remains attenuated in this range at TP 3 and TP 4 (Supplementary Figure 3).

3.2 Changes in stage 2 and SWS spectral features

Figure 2B replots the sleep data according to each stage to emphasize within-stage changes over time. By TP 4 in the stage 2 spectra, we identify a rightward shift in the spindle frequencies from ~8.5-9 to ~10-11 Hz (dark red lines). While these spindle frequencies at TP 4 post-CT-DBS do not reach the values of the peaks observed in the HV, they are trending towards the lower bound of expected spindling frequencies in healthy subjects (Figure 2A, right column). The SWS spectra (dark blue lines) demonstrate a complete suppression of the ~9 Hz abnormality at TP 2 for all channels and persisting thereafter (Supplementary Figure 3). The attenuation of this spindle peak in the SWS spectrum is more similar to the SWS features we observe in the HV (Figure 2A, right column).

Figure 2C shows the spindle peak frequency in stage 2 sleep and the peak power in the spindle range in SWS for all PS admissions across six fronto-central channels (F3, F4, FC5, FC6, C3, C4). For all channels shown, the spindle peak frequency value increases from the pre-CT-DBS time point to TP 2 post-CT-DBS (red lines). Three fronto-central channels (F3, F4, FC5) show increasing peak frequency from TP 2 to TP 3, with channels C3 and C4 remaining constant from TP 3 to TP 4 (red lines). The greatest increase in peak spindle frequency is seen in F3 and FC5 over the left frontal cortex. This is notable as the left frontal lobe demonstrates the most significant atrophy from the patient's diffuse axonal injury (Supplementary Figure 1). The peak power in the spindle range in SWS decreases on all channels from the pre-CT-DBS time point to TP 2 post-CT-DBS (blue lines).

3.3 Sleep scoring and time-frequency analyses

To further explore the large-scale sleep architecture, we characterized this PS' sleep via standard sleep scoring and nighttime time-frequency analyses. Figure 3 illustrates hypnograms of scored sleep stages and spectrograms obtained over the continuous time period marked by the hypnograms from a single frontal channel (Fp1-F3) in the PS and HV. Despite many arousals in the HV hypnogram, we note a cyclical pattern of progressively deeper sleep followed by bouts of REM, with SWS appearing in the beginning of the night (Figure 3A). This cycling through multiple stages of sleep that are easily defined in the EEG on visual inspection was absent at the pre-CT-DBS time point in the PS (Figure 3B).

The PS hypnogram at the pre-CT-DBS time point shows some sleep architecture that is not well-organized (Figure 3B). Specifically, we observe a large amount of fluctuation between stage 2 and SWS at multiple time intervals throughout the night that coincide with mixing of spectral features of both stage 2 and SWS in the pre-CT-DBS power spectra (Figure 2 A,B) as marked by brackets in Figure 3B. Sustained periods of stage 2 (predominantly spindling activity) and SWS (predominantly low frequency activity) were largely absent from the EEG record for the first time point. The total time spent in stage 1, stage 2, SWS, and REM was 238.5, 55.5, 52.5, and 0 minutes, respectively. The sleep efficiency index

(ratio between total sleep time and the amount of hours recorded) for the time point pre-CT-DBS was approximately 73%.

At TP 4, a greater amount of the overall EEG record is occupied by defined stage 2 and SWS (Figure 3C). Most notably, REM sleep emerged at TP 3 and remained present at TP 4 (Supplementary Figure 2). While the mixing of stages does not disappear entirely at TP 4, the emergence of REM produces an overall sleep architecture that is more typical of HV sleep. The total time spent in stage 1, stage 2, SWS, and REM was 189.5, 71.5, 66.5, and 5.5 minutes, respectively. From pre-CT-DBS to TP 4 post-CT-DBS, the amount of time spent in stage 2, SWS, and REM sleep increased by 16, 14, and 5.5 minutes, respectively. While the patient spent more time in stage 2, SWS, and REM at the post-CT-DBS time point, the sleep efficiency index was approximately 69%.

The amount of time spent in stage 1, stage 2, SWS, and REM for one night of HV sleep was 55, 237, 50.5, and 79 minutes, respectively. The sleep efficiency index for the HV was 87.5%. For HVs, normal sleep efficiency is approximately 80%. The amount of time spent in stage 2 and SWS at the post-CT-DBS time point (71.5 and 66.5 minutes, respectively) are trending towards the values observed in a HV.

4. Discussion

Our findings demonstrate late changes in sleep dynamics that may be temporally associated with the introduction of daily cyclic CT-DBS 21-years after severe structural brain injury. Prior to CT-DBS, the patient demonstrated a rare and constant mixing of stage 2 and SWS features that separated into distinct stage 2 and SWS states at one year after implantation (Supplementary Figure 3). Progressive changes in sleep dynamics over the next three years included increases in spindle frequency and the attenuation of an abnormal spindle peak in SWS (Figure 2), as well as the emergence of REM sleep at TP 3 and TP 4 (Figure 3C, Supplementary Figure 2). These changes are remarkable in the context of their very late post-injury emergence and the degree of structural brain injury present in this patient. We consider the potential underlying mechanisms linking CT-DBS during the wakeful state to these observed alterations in sleep dynamics measured in the EEG.

While this study was not designed to causally verify a relationship between CT-DBS implantation and the alterations of sleep features and sleep architecture, it is parsimonious to associate this with CT-DBS for the following reasons: 1) the long-time course of brain injury before stimulation, and 2) the population expectation that as healthy subjects and patients with neurodegenerative diseases age, their sleep architecture, specifically spindling, SWS, and REM activity, should decline (Feinberg 1974; Wauquier 1993; Crowley et al. 2002; Petit et al. 2004). Here we have observed the opposite effect in our

PS, who exhibited increases in spindle frequency in stage 2 sleep, the amount of sustained SWS, and the reemergence of REM sleep starting at TP 3 post-CT-DBS.

We suggest two interdependent mechanisms to account for how CT-DBS may have modulated sleep processes in this PS. Firstly, daytime CT-DBS may *indirectly* affect sleep processes due to increased cortical activity during the day. Second, daytime CT-DBS may *directly* alter sleep features because it drives thalamocortical pathways that play a role in the generation stage 2 and SWS elements. The evidence of the former is well-known (Huber et al. 2004; Tononi and Cirelli 2006a; Vyazovskiy et al. 2009).

Why would CT-DBS during the day influence sleep processes? Changes in SWS in particular have been proposed to be influenced by wakeful activities. At the cellular level, Tononi & Cirelli (2006) have hypothesized that activity-dependent changes during the day have the ability to modulate SWS. In an animal model, it has been shown that average cortical firing rates in NREM and REM sleep increase after sustained wakefulness or activity during the day (Vyazovskiy et al. 2009). Moreover, human subjects who engaged in a region-specific learning task showed increases in sleep delta power from 1-4 Hz. This increase in SWS was correlated with better performance on the task after sleep (Huber et al. 2004). High frequency CT-DBS strongly modulates synaptic input within the thalamus, striatum, and frontal cortices (Liu et al. 2015). Thus, continuous CT-DBS over a 12-hour period as in our PS can be interpreted to approximate the effects of increased wakefulness by its direct depolarizing effects on neurons across the frontal cortex and striatum. Similarly, REM sleep requires the strong depolarization of neuronal populations (Mircea and Robert 2005). The late emergence of REM at three years after the onset of CT-DBS suggests that the requirements for overall activity may have been higher than those producing changes in Stage 2 and SWS. Given these findings, we propose that broad activation of fronto-striatal activity during the day may be a unifying mechanism for the changes observed in both sleep stages in our patient and in the emergence of a more complete sleep architecture.

We next consider the direct effect that CT-DBS could have on the modulation of sleep features. The physiological mechanisms for spindle and slow wave generation overlap with the fronto-striatal regions that are strongly driven by CT-DBS (Contreras et al. 1997; David et al. 2013). While CT-DBS was only on during the day, this type of stimulation has been shown to demonstrate carry-over effects on behavioral facilitation (Schiff et al. 2007). Spindling activity in stage 2 sleep has been shown to correlate with behavioral recovery in stroke patients as well as in patients recovering from traumatic brain injury (Gottselig, Bassetti, & Achermann 2002; Urakami 2012; Forgacs et al. 2014). Gottselig, Bassetti, & Achermann (2002) conducted within-subject comparisons from thirty stroke patients during the acute, sub-chronic, and chronic stages of recovery, and found that patients in the chronic phase of recovery demonstrated significant increases in the power and coherence of sleep spindle frequency activity.

Similarly, Forgacs et al. (2014) demonstrated that preservation of spindles in patients with severe brain injuries correlated with higher levels of cognitive recovery as measured using neuroimaging techniques. The changes in stage 2 spindle frequency measured here are thus comparable to findings in spontaneous recovery following stroke and other types of structural brain injury and therefore consistent with the proposed role of changes in the brain typically associated with increased wakeful behaviors.

Collectively, our findings suggest that late, long-term modification of sleep mechanisms can arise in the severely injured brain in the absence of overt behavioral improvements. These data propose that tracking sleep recovery in patients with disorders of consciousness may provide an independent assay to test the spontaneous recovery of brain function over time or possibly, the efficacy of interventions. Preliminary studies show evidence of similar changes in patients with disorders of consciousness studied longitudinally who demonstrate spontaneous improvements (Thengone et al., 2011). Thus, our findings, although restricted to a single subject, support both the general hypothesis of synaptic homeostasis in sleep (Tononi and Cirelli 2006a) and also the potential role of sleep in establishing long-term, late plastic changes in the structurally injured brain.

References

American Clinical Neurophysiology Society. Guideline 7: Guidelines for writing EEG reports. J Clin Neurophysiol 2006; 23:118–121

Bokil H, Andrews P, Kulkarni JE, Mehta S, Mitra PP. Chronux: A platform for analyzing neural signals. J Neurosci Methods. 2010;192(1):146–51.

Cologan V, Schabus M, Ledoux D, Moonen G. Sleep in disorders of consciousness. Sleep Med. 2010;14(2):97–105.

Contreras D, Destexhe a, Sejnowski TJ, Steriade M. Spatiotemporal patterns of spindle oscillations in cortex and thalamus. J Neurosci. 1997;17(3):1179–96.

Crowley K, Trinder J, Kim Y, Carrington M, Colrain IM. The effects of normal aging on sleep spindle and K-complex production. Clin Neurophysiol. 2002;113(10):1615–22.

David F, Schmiedt JT, Taylor HL, Orban G, Di Giovanni G, Uebele VN, et al. Essential Thalamic Contribution to Slow Waves of Natural Sleep. J Neurosci [Internet]. 2013;33(50):19599–610. Available from: http://www.jneurosci.org/cgi/doi/10.1523/JNEUROSCI.3169-13.2013

Feinberg I. Changes in sleep cycle patterns with age. J Psychiatr Res. 1974;10(3-4):283–306.

Forgacs PB, Conte MM, Fridman E a, Voss HU, Victor JD, Schiff ND. Preservation of electroencephalographic organization in patients with impaired consciousness and imaging-based evidence of command-following. Ann Neurol [Internet]. 2014;76(6):869–79. Available from: http://www.pubmedcentral.nih.gov/articlerender.fcgi?artid=4354809&tool=pmcentrez&rendertype=

abstract

Frigo M, Johnson SG. The design and implementation of FFTW3. Proc IEEE. 2005. p. 216–31.

Giacino JT, Fins JJ, Machado A, Schiff ND. Central Thalamic Deep Brain Stimulation to Promote Recovery from Chronic Posttraumatic Minimally Conscious State: Challenges and Opportunities. Neuromodulation Technol Neural Interface [Internet]. 2012;15(4):339–49. Available from: http://doi.wiley.com/10.1111/j.1525-1403.2012.00458.x

Giacino JT, Kathleen K, John W. The JFK Coma Recovery Scale--Revised: Measurement characteristics and diagnostic utility. Archives of Physical Medicine and Rehabilitation. 2004;85(12):2020-2029.

Giacino JT, Ashwal S, Childs N, Cranford R, Jennett B, Katz DI. The minimally conscious state. Neurology. 2002;58(3):349–53.

Gold L, Lauritzen M. Neuronal deactivation explains decreased cerebellar blood flow in response to focal cerebral ischemia or suppressed neocortical function. Proc Natl Acad Sci [Internet]. 2002;99(11):7699–704. Available from: http://www.pnas.org/cgi/doi/10.1073/pnas.112012499

Gottselig JM, Bassetti CL, Achermann P. Power and coherence of sleep spindle frequency activity following hemispheric stroke. Brain [Internet]. 2002;125(2):373–83. Available from: http://www.brain.oxfordjournals.org/cgi/doi/10.1093/brain/awf021

Huber R, Felice Ghilardi M, Massimini M, Tononi G. Local sleep and learning. Nature [Internet]. 2004;430(6995):78–81. Available from: http://www.nature.com/doifinder/10.1038/nature02663\npapers3://publication/doi/10.1038/nature02663

Landsness E, Bruno M-A, Noirhomme Q, Riedner B, Gosseries O, Schnakers C, et al. Electrophysiological correlates of behavioural changes in vigilance in vegetative state and minimally conscious state. Brain [Internet]. 2011;134(8):2222–32. Available from: http://www.brain.oxfordjournals.org/cgi/doi/10.1093/brain/awr152

Liu J, Lee HJ, Weitz AJ, Fang Z, Lin P, Choy M, et al. Frequency-selective control of cortical and subcortical networks by central thalamus. Elife. 2015;4(DECEMBER2015).

Mircea S, Robert MW. Brain control of Wakefulness and sleep [Internet]. Vasa. 2005. Available from: http://medcontent.metapress.com/index/A65RM03P4874243N.pdf

Mitra PP, Pesaran B. Analysis of dynamic brain imaging data. Biophys J [Internet]. 1999;76(2):691–708. Available from: http://www.pubmedcentral.nih.gov/articlerender.fcgi?artid=1300074&tool=pmcentrez&rendertype=abstract\nhttp://www.ncbi.nlm.nih.gov/pubmed/9929474

Mölle M, Bergmann TO, Marshall L, Born J. Fast and slow spindles during the sleep slow oscillation: disparate coalescence and engagement in memory processing. Sleep [Internet]. 2011;34(10):1411–

21. Available from: http://www.pubmedcentral.nih.gov/articlerender.fcgi?artid=3174843&tool=pmcentrez&rendertype=abstract

Schiff ND. Moving toward a generalizable application of central thalamic deep brain stimulation for support of forebrain arousal regulation in the severely injured brain [Internet]. Vol. 1265, Annals of the New York Academy of Sciences. 2012. p. 56–68. Available from: http://www.embase.com/search/results?subaction=viewrecord&from=export&id=L365455038\nhttp://dx.doi.org/10.1111/j.1749-6632.2012.06712.x\nhttp://mgetit.lib.umich.edu/sfx_locater?sid=EMBASE&issn=00778923&id=doi:10.1111/j.1749-6632.2012.06712.x&atitle=Moving

Percival DB, Walden AT. Spectral Analysis for Physical Applications: Multitaper and Conventional Univariate Techniques. Vol. 38, Cambridge Cambridge University Press. 1993.

Petit D, Gagnon JF, Fantini ML, Ferini-Strambi L, Montplaisir J. Sleep and quantitative EEG in neurodegenerative disorders. Vol. 56, Journal of Psychosomatic Research. 2004. p. 487–96.

Schiff ND. Recovery of consciousness after brain injury: a mesocircuit hypothesis. Vol. 33, Trends in Neurosciences. 2010. p. 1–9.

Schiff ND, Giacino JT, Kalmar K, Victor JD, Baker K, Gerber M, et al. Behavioural improvements with thalamic stimulation after severe traumatic brain injury. Nature [Internet]. 2007;448(7153):600–3. Available from: http://www.nature.com/doifinder/10.1038/nature06041

Thengone, DJ, Teslovich, T, Conte, MM, Victor, JD, Schiff, ND. Tracking longitudinal spectral changes in wake and sleep EEG in severe brain injury. Program No. 675.08. 2011. Neuroscience Meeting Planner. Washington, DC: Society for Neuroscience, 2011. Online.

Thomson DJ. Spectrum estimation and harmonic analysis. Proc IEEE [Internet]. 1982;70(9):1055–96. Available from: http://ieeexplore.ieee.org/xpl/login.jsp?tp=&arnumber=1456701&url=http%3A%2F%2Fieeexplore.ieee.org%2Fxpls%2Fabs_all.jsp%3Farnumber%3D1456701

Tononi G, Cirelli C. Sleep function and synaptic homeostasis. Vol. 10, Sleep Medicine Reviews. 2006a. p. 49–62.

Urakami Y. Relationship Between Sleep Spindles and Clinical Recovery in Patients With Traumatic Brain Injury: A Simultaneous EEG and MEG Study. Clin EEG Neurosci [Internet]. 2012;43(1):39–47. Available from: http://eeg.sagepub.com/lookup/doi/10.1177/1550059411428718

Voss HU, Ulŭg AM, Dyke JP, Watts R, Kobylarz EJ, McCandliss BD, et al. Possible axonal regrowth in late recovery from the minimally conscious state. J Clin Invest. 2006;116(7):2005–11.

Vyazovskiy V V., Olcese U, Lazimy YM, Faraguna U, Esser SK, Williams JC, et al. Cortical Firing and

Sleep Homeostasis. Neuron. 2009;63(6):865–78.
Wauquier A. Aging and changes in phasic events during sleep. Physiol Behav. 1993;54(4):803–6.

Figure Legends

Figure 1. Timeline of patient data collection.

Study timeline and main findings. 10-second EEG segments are displayed for pre-CT-DBS and post-CT-DBS (TP 4) time points. **Left**: red arrow designates a "stage 2-like" sleep at the pre-CT-DBS time point, with slow and partially formed spindles. Blue arrow points to a "SWS-like" stage, with the intrusion of stage 2-like elements and slow spindles within slow wave activity. **Right**: red arrow highlights stage 2 sleep at TP 4 post-CT-DBS containing faster spindling activity. Blue arrow illustrates SWS at TP 4; segments contain increased low frequency activity and fewer stage 2-like elements. See Supplementary Figure 3 to view power spectra (as described in the blue and red boxes) at each time point.

Figure 2. Stage 2 and SWS dynamics pre- and post-CT-DBS in the PS and HV.

Examples of representative EEG responses from the PS in comparison with the HV. **A:** power spectra responses recorded from channels F3 and F4 at two time points (pre-CT-DBS and TP 4 post-CT-DBS) for both stage 2 (red) and SWS (blue) as compared to the HV. **B:** power spectra from stage 2 (red) and SWS segments (blue) obtained from pre-CT-DBS (light red or blue) and post-CT-DBS (TP 4) (dark red or blue) time points plotted on one axis. Double-headed arrow and brackets denote the lower (12 Hz) and upper (15 Hz) bounds of spindling activity observed in healthy sleep (Mölle, Bergmann, Marshall, & Born, 2011). By TP 4, the spindle peak frequency is approaching the lower bound of this range. **C:** center spindle peak frequency in stage 2 sleep and the peak power in the spindle range in SWS for each study time point across channels F3, F4, FC5, FC6, C3, and C4. These values were determined after normalization using the method from Gottselig, Bassetti, & Achermann (2002) (see Methods).

Figure 3. Time-varying spectrograms and hypnograms.

Time-varying spectrograms and hypnograms were calculated from bipolar channel Fp1-F3 for pre- and post-CT-DBS implantation (TP 4) conditions, and for the HV. In the hypnograms, the x-axis indicates continuous time (10PM to 6AM), and the y-axis indexes sleep stages. **A:** HV spectrogram and accompanying hypnogram. **B:** spectrogram and hypnogram from the pre-CT-DBS time point. Red brackets in spectrogram indicate a mixing of stages, with low frequency (delta waves) co-occurring with

higher frequency elements (spindle-like peaks). The sleep stage labels in B are denoted as "Stage 2-like" and "SWS-like" to emphasize that isolated stages of sleep were difficult to discern via standard visual scoring. **C:** At TP 4 post-CT-DBS, more defined stage 2 and SWS dominated the EEG record. However, there were still individual epochs that contained the mixing of sleep features. REM sleep emerged at TP 3 and remained present at TP 4 (Supplementary Figure 2).

Supplementary Figure 1. T1 Weighted MRI horizontal brain images.

Four representative T1 weighted horizontal brain images are shown illustrating left greater than right atrophy secondary to severe diffuse axonal injury.

Supplementary Figure 2. Sample EEG tracings of REM sleep.

7-second EEG tracings of representative REM sleep from the PS at (**A**) TP3 and (**B**) TP4 post-CT-DBS, segments from ~11 PM and 2AM, respectively. Red boxes show EOG artifacts on anterior frontal channels appearing with lateralized eye movements that correlate with direct EOG measurement (TP 4 only).

Supplementary Figure 3. Power spectral changes in stage 2 and SWS across all study time points.

Power spectral responses from channel F3 of representative stage 2 (red) and SWS (blue) for pre-CT-DBS and each post-CT-DBS (TP 2, TP 3, TP4) time point. Note the loss of the spindle peak that occurs at the first time point post-CT-DBS (TP 2).

Figure 1

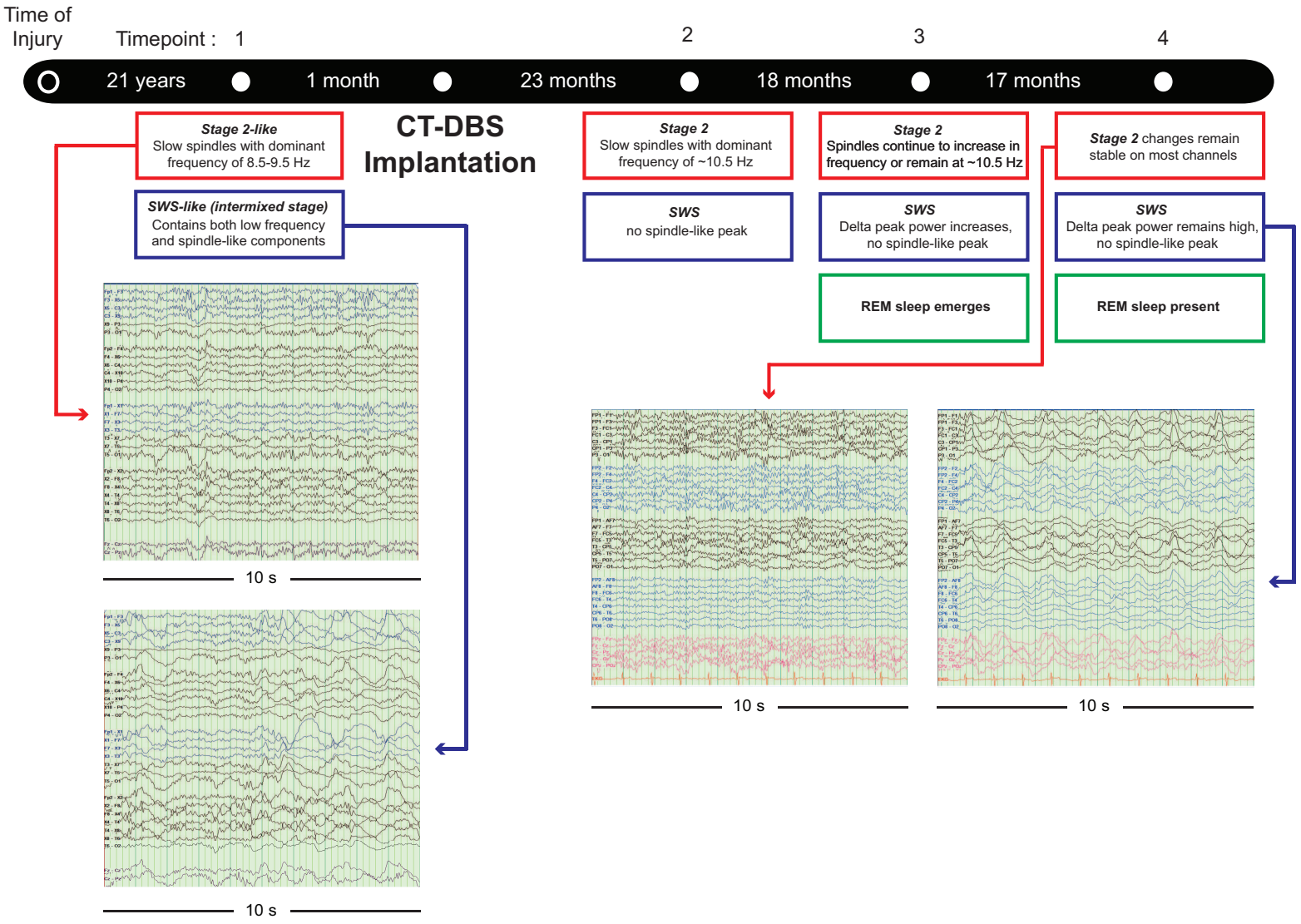

Figure 1

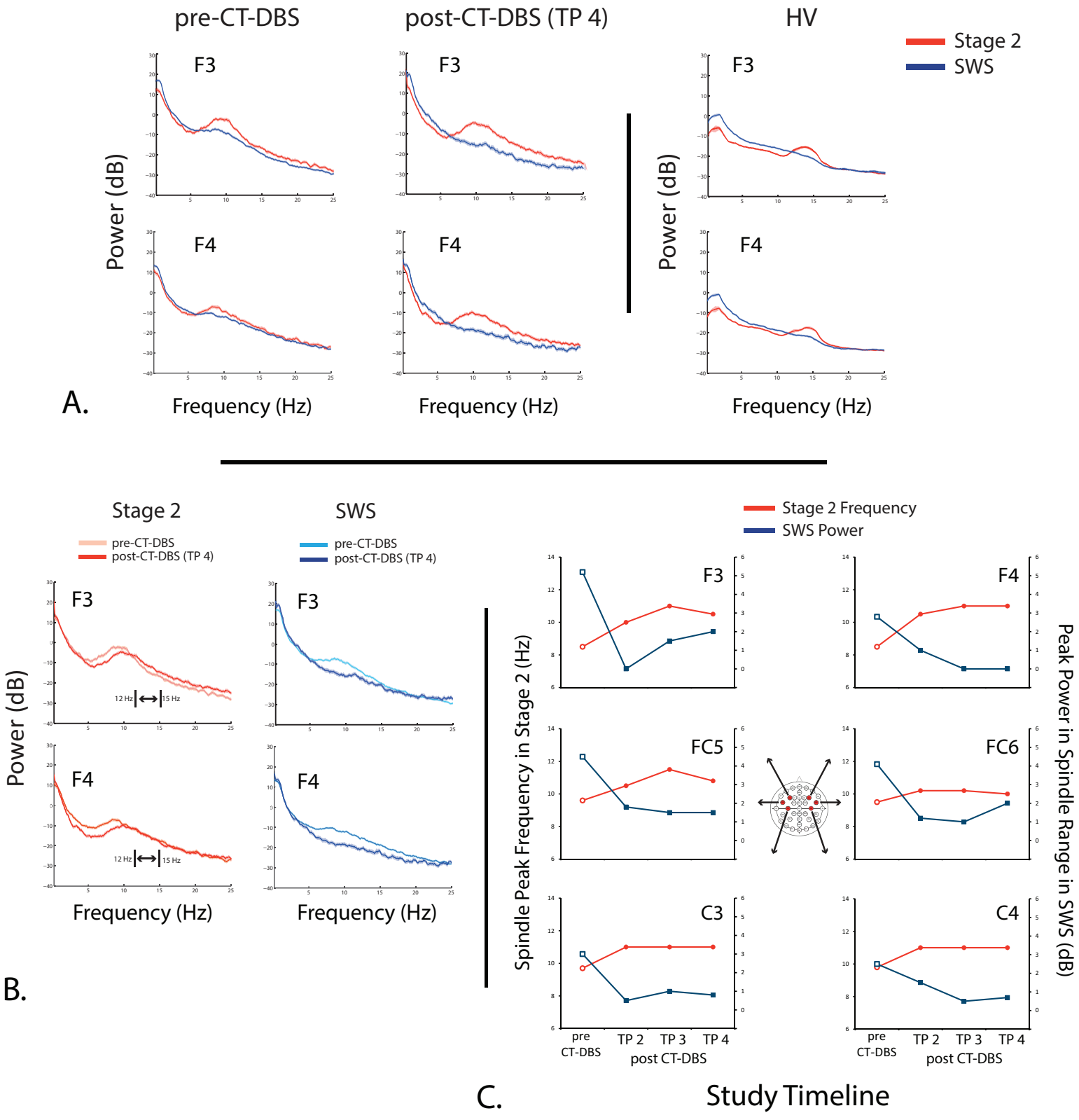
pre-CT-DBS
post-CT-DBS (TP 4)
HV
Stage 2
SWS
F3
F4
Power (dB)
Frequency (Hz)
A.
Stage 2
SWS
pre-CT-DBS
post-CT-DBS (TP 4)
12 Hz
15 Hz
B.
Stage 2 Frequency
SWS Power
Spindle Peak Frequency in Stage 2 (Hz)
Peak Power in Spindle Range in SWS (dB)
FC5
FC6
C3
C4
pre CT-DBS
TP 2
TP 3
TP 4
post CT-DBS
C.
Study Timeline

HV

Fp1 - F3

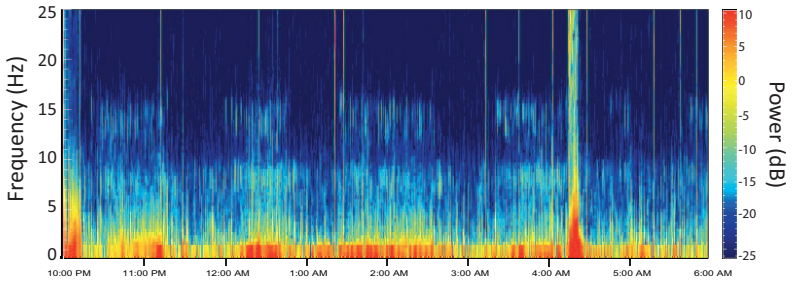

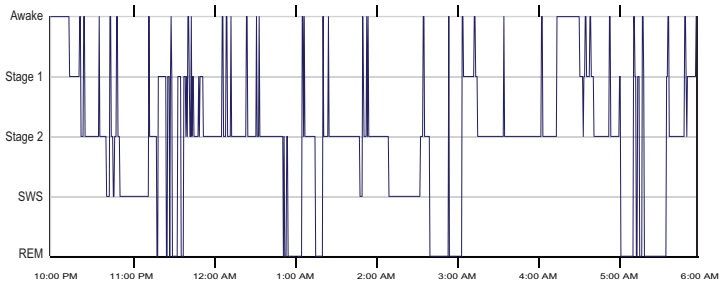

A.

PS

pre CT-DBS

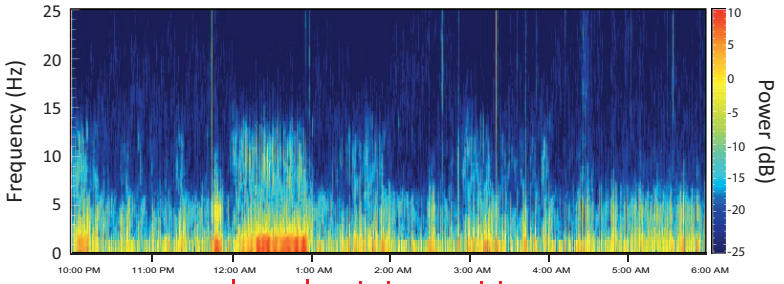

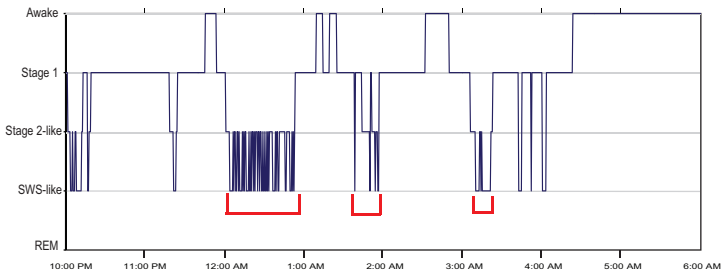

B.

post CT-DBS (TP 4)

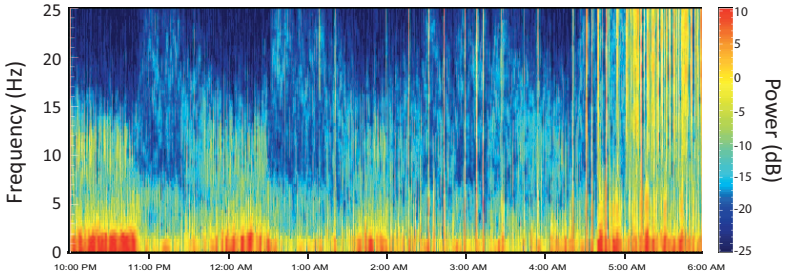

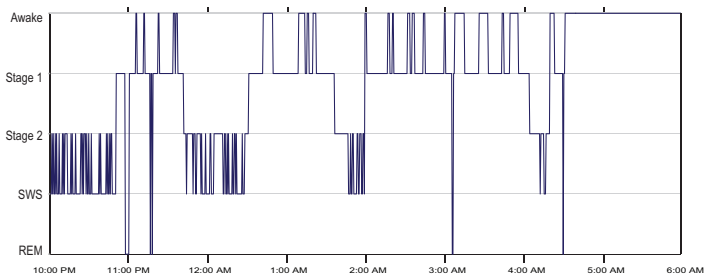

C.

Supplement A. Clinical history.

Patient is a 44 year old male who suffered a severe traumatic brain injury in a motor vehicle accident at the age of 17. Initial brain imaging at the time of injury showed evidence of a small left thalamic hemorrhage consistent with diffuse axonal injury. Patient has remained unable to communicate or respond to spoken commands since the time of the injury. Neurological examination on first examination at the time of the study notable for a dense right hemiparesis and contracture of the right upper extremity. Cranial nerve examination: no blink to threat, scanning eye movements without fixation, positive corneal reflexes and gag reflex. Motor examination notable for diffuse hypertonicity with withdrawal to noxious stimuli in right upper extremity only. Tendon reflexes showed hyporeflexia in right upper extremity and hyperreflexia in right lower extremity. Bilateral extensor plantar signs were present. Notably, the patient demonstrated evidence of emotional reactivity to humorous or scatological speech despite no consistent purposeful movements of head, eyes, or limbs. Quantitative behavioral assessments of the patient using the Coma Recovery Scale-Revised (Giacino et al. 2004) done beginning at the first research evaluation at age 38 were consistent with minimally conscious state based on contingent emotional reactivity (consistent laughter to selective stimuli) and responsive vocalizations. Total CRS-R scores remained in the range 12-14 over the four years of assessments during the time period of the reported sleep-wake studies here. Average subscale scores of CRS-R: Auditory (2); Visual (1); Motor (5); Oromotor (2); Communication (0); Arousal (2). Despite continuous CT-DBS over the time period of the present study no consistent qualitative behavioral change was documented and CRS-R scores remain in the same range.

Supplementary Figure 1

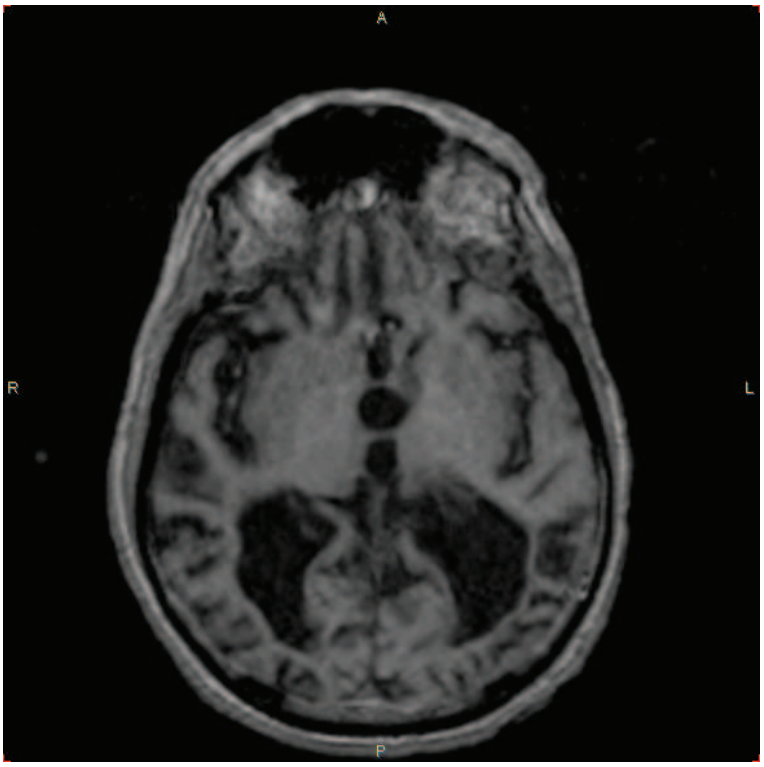

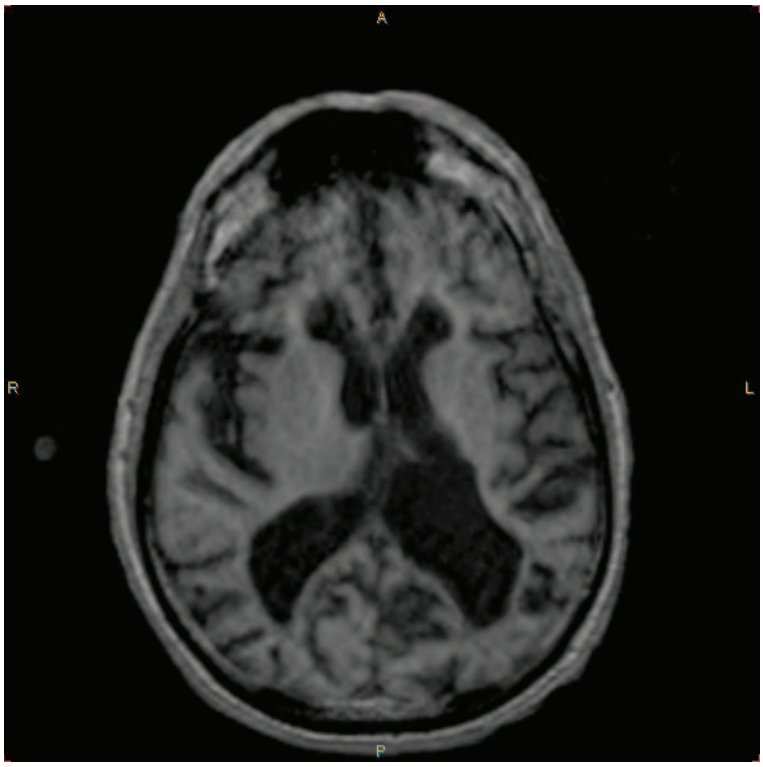

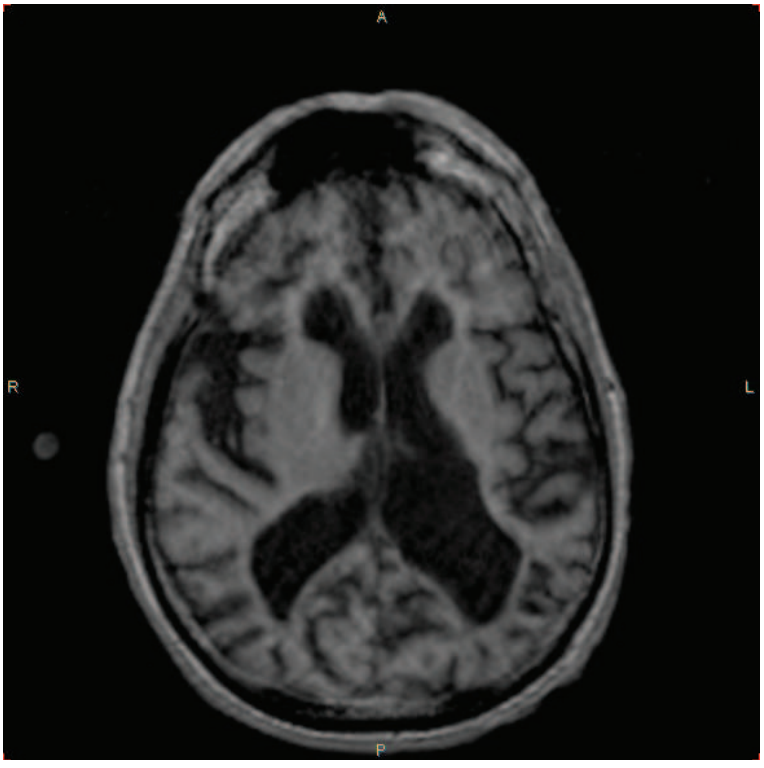

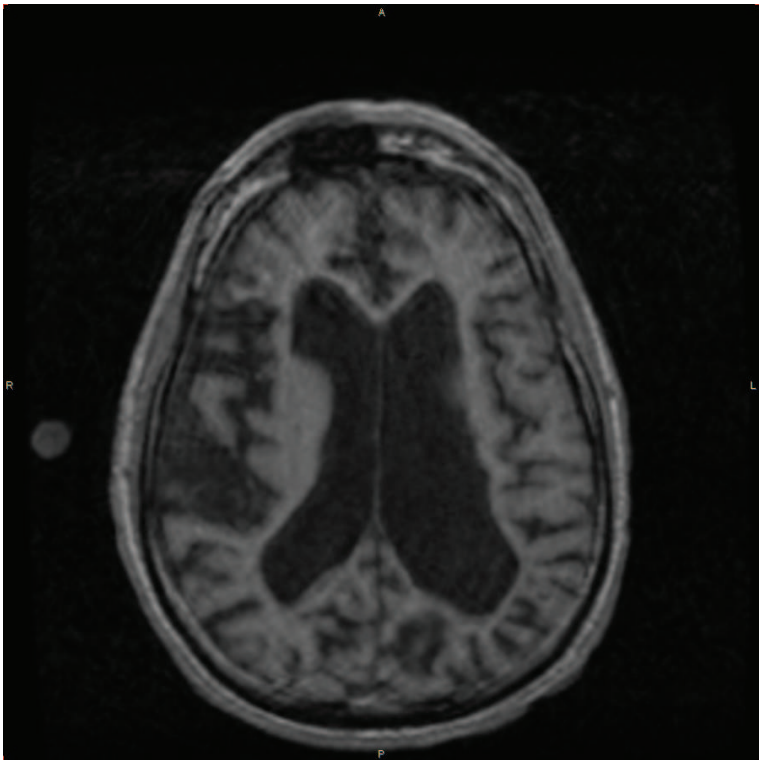

Supplementary Figure 1

Supplementary Figure 2

TP 3 post-CT-DBS

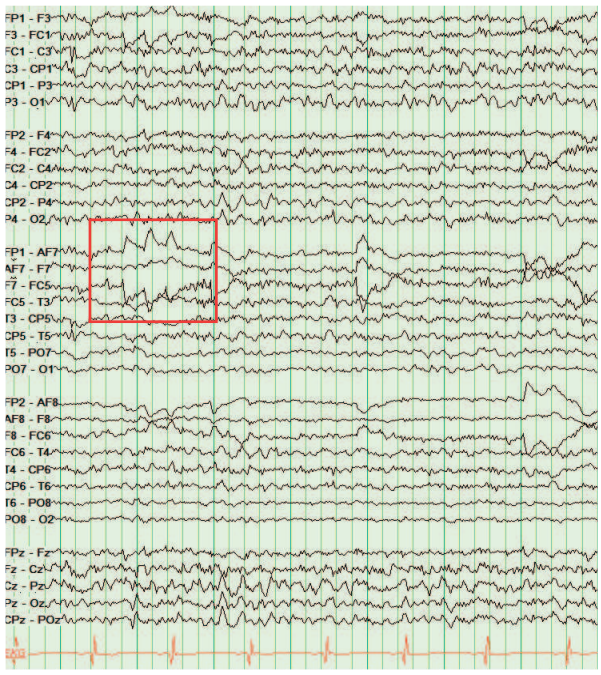

TP 4 post-CT-DBS

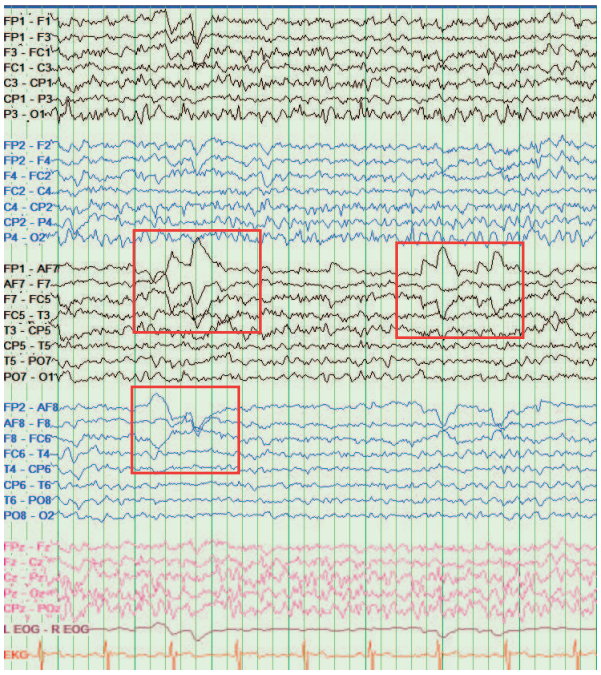

Supplemental Figure 2

Supplementary Figure 3

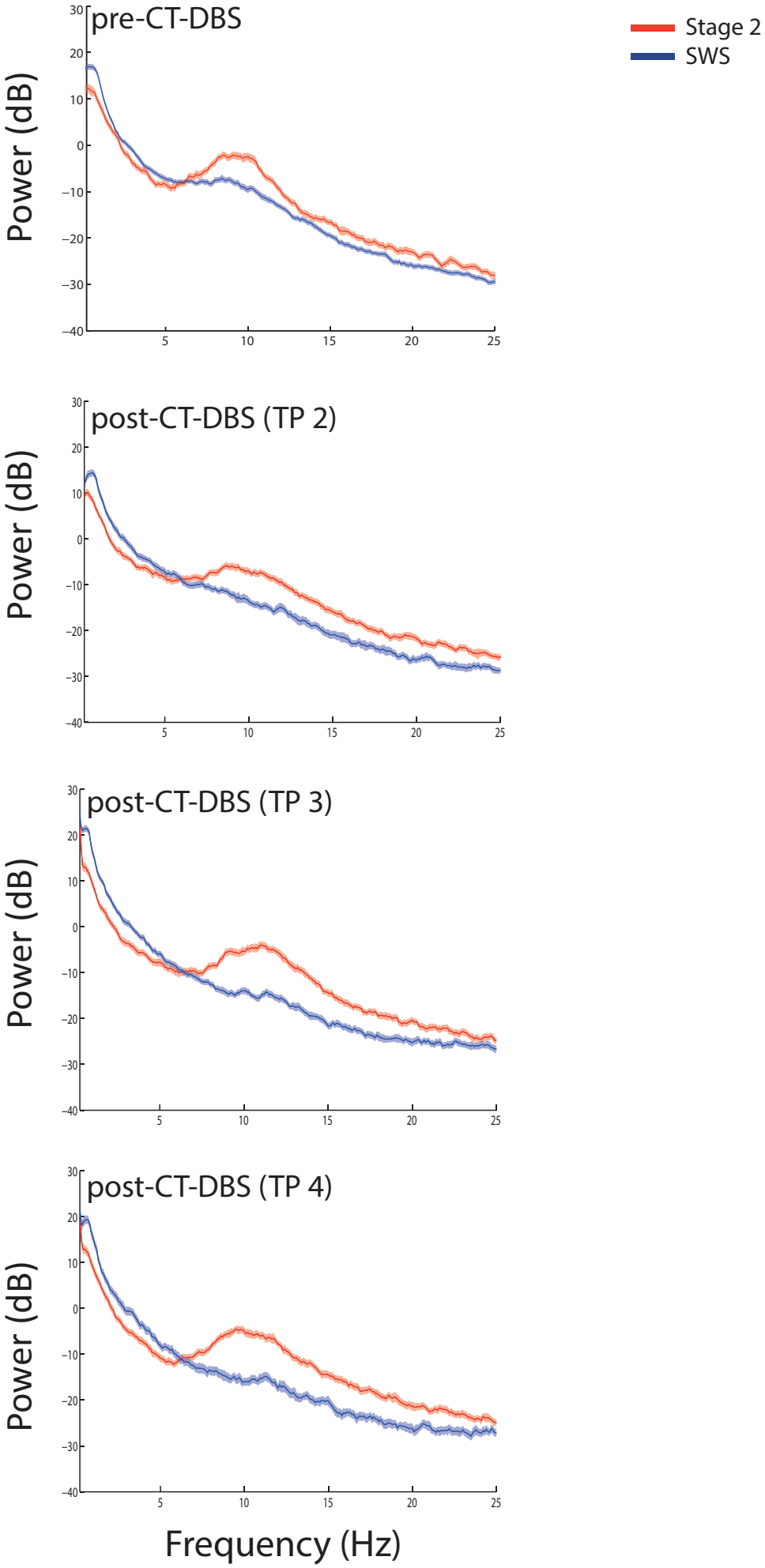

Supplemental Figure 3